ELSEVIER

Journal of Hydrology 242 (2001) 64–78

Journal of Hydrology

www.elsevier.com/locate/jhydrol

Laboratory measurement of water imbibition into low-permeability welded tuff

M.Q. Hu*, P. Persoff, J.S.Y. Wang

1 Cyclotron Road, MS 90-1116, Earth Sciences Division, Lawrence Berkeley National Laboratory, Berkeley, CA 94720, USA

Received 28 July 1999; revised 27 April 2000; accepted 11 October 2000

Abstract

Laboratory imbibition and vapor-diffusion experiments were developed and conducted to measure accurately water imbibition and vapor condensation into welded tuff of low permeability. Automatically recorded balance readings were used to quantify the uptake of water into rock cores by imbibition and/or vapor condensation. The total uptake of water was checked against independent weighings of the sample before and after each experiment. As water was imbibed into the sample and evaporated from the reservoir, the buoyant force on the sample decreased. Balance readings corrected for the buoyancy effect agreed very well with independently measured total uptake. Sorptivity was calculated from the slope of a plot of corrected cumulative imbibition versus square-root of time. Vapor condensation can provide a significant contribution to the water uptake into cores during imbibition experiments. Rock cores were coated with epoxy on the sides and covered on the top (except for a small hole that allowed air to escape) to minimize the vapor condensation contribution. Comparison of the sorptivity values between different core treatments shows that a consistent fraction, about 20%, of water uptake actually enters the core by vapor condensation. Overall, methods for separating the confounding effects of buoyant-force change and vapor condensation result in more accurate measurement of sorptivity, as exhibited by the consistent and reproducible results of triplicate measurements. These methods for buoyancy and vapor-condensation correction are expected to be very useful for measuring imbibition rates on a wide range of porous materials, especially very-low-permeability materials.

Keywords: Imbibition; Sorptivity; Capillarity; Vapor diffusion; Buoyancy

1. Introduction

Fracture flow, fracture–matrix interaction, and matrix imbibition are key processes in flow and transport through the unsaturated zone at Yucca Mountain, Nevada, the only site currently under consideration for a US Department of Energy underground high-level radioactive waste repository. As water infiltrates down from the ground surface through the fracture network, some water may be imbibed from the flowing fractures into the matrix rock. As long as the matrix rock is unsaturated, a capillary driving force exists for the imbibition process. The partitioning of water between matrix imbibition and fracture flow is very important for the design and performance of a potential repository at Yucca Mountain.

The rate of imbibition is determined by the product of a driving force and conductivity. The driving force is the gradient of moisture tension between the matrix and the fracture, and the conductivity is the unsaturated hydraulic conductivity of the matrix rock. At

* Corresponding author. Fax: +1-510-486-5686.
E-mail address: q_hu@lbl.gov (M.Q. Hu).

0022-1694/01/$ - see front matter
PII: S0022-1694(00)00388-7

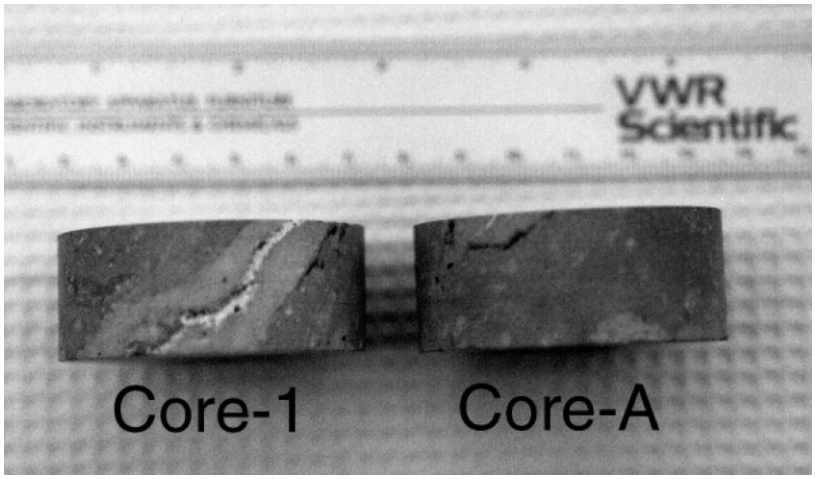

Fig. 1. Photograph showing unfractured Core A and fractured Core 1 (with an altered zone surrounding the fracture).

low liquid saturation, the driving force is high, but the unsaturated hydraulic conductivity is low. At high saturation, the reverse is true. Because the pores in welded tuff are extremely small, the driving force for imbibition and resistance to flow can both be extremely large. Roberts and Lin (1997) measured pore size distributions of tuff from the Topopah Spring member of the Paintbrush formation at Yucca Mountain by mercury porosimetery and found average pore diameters (weighted by increments of pore space filled) of 53.1 nm and 19.7–21.4 nm for welded and densely welded samples, respectively. When such small pores are unsaturated, moisture can be under extremely high tension, and the intrinsic permeability k (and saturated hydraulic conductivity K_{sat}) of these materials can be very small. The measured saturated hydraulic conductivity for rock matrix of the Topopah Spring welded (TSw) units ranges from 4.0×10^{-11} to 1.7×10^{-9} m s^{-1} (Flint, 1998).

Sorptivity, which is jointly controlled by the capillary pressure and permeability, quantifies the rate of imbibition. The sorptivity is a useful parameter for characterizing transient imbibition processes, especially when the influence of gravity is insignificant. To define sorptivity, consider a semi-infinite, homogeneous, one-dimensional medium into which water is imbibed at one end. The cumulative uptake of water by imbibition is given by Philip (1957) as:

$$I(t) = St^{0.5} + At \quad (1)$$

where $I(t)$ is cumulative imbibition (m) as a function of time, t is time (in seconds, s), S the sorptivity (m s$^{-0.5}$), which is a function of the initial and boundary water contents, and A (m s^{-1}) is an empirically determined constant that depends upon the medium properties, initial water content, and boundary conditions (Jury et al., 1991). According to Philip (1957), the term At is negligible when the gravity potential gradients are small relative to matric potential gradients. Under this condition, which is applicable for our tests, the slope of $I(t)$ versus $t^{0.5}$ is the sorptivity S. Gravitational effects can be ignored if the sample length is much less than the "sorptive length", which is a property of the rock. Zimmerman et al. (1990) showed that the sorptive lengths of Yucca Mountain tuffs are typically a few meters, compared to 0.02 m sample length of cores used in this study.

As pointed out by Humphrey et al. (1996), measurement of sorptivity permits estimation of two characteristic functions, relative permeability and capillary pressure curve. The difficulty of measuring the characteristic functions in low-permeability rocks has encouraged the use of various algorithms that enable estimation of these functions from more readily measurable properties, such as sorptivity (Zimmerman et al., 1993; Zimmerman and Bodvarsson, 1995). The objective of this work is to improve (by providing a mathematical correction for the buoyant-force change) an established measurement method such that small sorptivity value can be accurately

Table 1
Types of experiments and core treatments

Tests	Case 1	Case 2	Case 3
Imbibition (WI)	No coating[a]	Sides epoxy-coated[b]	Sides epoxy-coated and top covered with foil
Condensation (VDC)	Core bottom and 1-mm of the side covered with aluminum foil, secured by wire.	Bottom foil-covered and sides epoxy-coated	Sides epoxy-coated; bottom and top foil-covered, with a 2-mm hole in the top

[a] Similar to unjacketed tests of Humphrey et al. (1996).
[b] Similar to jacketed tests of Humphrey et al. (1996), who used heat-shrink tubing; we painted the sides with a five-minute epoxy and verified complete coverage by visual inspection.

measured. The well-established sorptivity measurement approach has been extensively reviewed by Humphrey et al. (1996).

In this work, we have measured sorptivity of tuff cores with and without fractures and have introduced corrections for previously unnoticed, but significant, sources of error: the change in buoyancy force during imbibition, and water uptake by vapor diffusion. These sources of error become significant for samples of low available porosity (resulting in small weight gain) or low sorptivity (requiring long duration for the experiment).

2. Materials and methods

2.1. Rock samples

Rock cores 5.08 cm in diameter and 2.0 cm in length (except L4 which was 4.0 cm long) were cut and machined from a sample block collected from the TSw unit at Yucca Mountain. Cores identified by letters (i.e. A, B, C, M, L2 and L4) have no visible fractures, while cores identified by numbers (i.e. 1 and 2) have visible fractures with fillings surrounded by an altered zone (Fig. 1). Dry core weights were obtained after oven drying to constant weight. All cores used for the imbibition experiments were initially dried at 60°C, except Core M, which was partially saturated by equilibrating it within a relative humidity chamber until it reached constant weight. Porosity, bulk volume, and bulk density were determined by weighing the sample dry, vacuum-saturated, and saturated-and-submerged (the method of Archimedes).

2.2. Water uptake measurements

Two types of water uptake experiments were done: water imbibition (WI) experiments, in which the sample was in contact with liquid water, and vapor diffusion and condensation (VDC) experiments, in which the sample was suspended above the water surface.

2.3. Water imbibition measurements

To measure imbibition rates into cores, we suspended the rock core from a bottom-weighing electronic balance, with its machined-flat bottom end horizontal. The rock core was located inside a chamber with a reservoir (a glass Petri dish) resting on its floor. The humidity in the chamber was less than 100% (measured to be above 94%) because of the open hole in the chamber to let the suspension wire to pass through. The chamber could be raised or lowered on a support jack to bring the rock core in contact with water in the reservoir, submerged to about 1 mm depth. Balance readings were automatically recorded as frequently as once per second. The temperature was maintained at 22.5 ± 0.5°C. During the WI experiments, the position of the wetting front along the length of the outside of the core was visually observed.

Before each run, we weighed each sample, the empty reservoir, and the reservoir with its initial content of water. At the end of the run, the sample was lifted out of the reservoir, excess surface water was absorbed into a tared moist Kimwipe, and the sample and Kimwipe were weighed separately. The weight changes of the core and the reservoir were

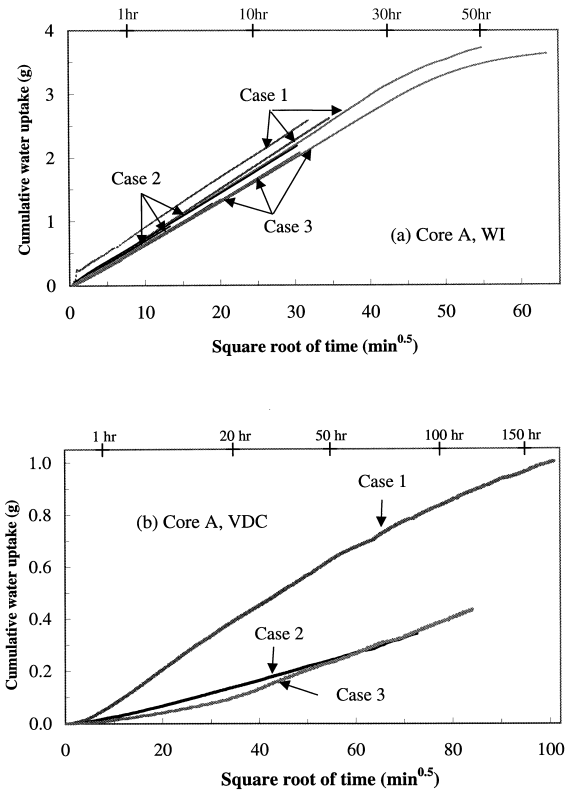

Fig. 2. Cumulative water uptake from balance indicated weights vs. the square root of time for unfractured Core A: (a) WI experiments, three cases in triplicate. (b) VDC experiments, three cases.

measured for mass-balance analysis. Water unaccounted for was treated as the evaporative loss over the experiment duration. A blank experiment without any sample was done to confirm the estimated evaporative loss.

All imbibition measurements were repeated in triplicate on the same sample. Between runs, the sample was dried with the same procedure. Repeated measurement of oven dry weight agreed within 0.01 g (less than a 3% change in full saturation). Triplicate imbibition measurements were also done on all samples with different parts of the cores coated or covered to inhibit vapor-phase uptake. Table 1 summarizes the three cases of core treatments for the experiments.

2.4. Correction for effects of buoyancy on imbibition measurements

The cumulative mass of water imbibed into the core indicated by balance readings was always greater than the weight gain of the core sample calculated from independent weighings at the beginning and end of the experiment. This weight check thus revealed a source of error that has not been explicitly accounted for by previous investigators. As the sample imbibed water, the water level in the reservoir fell and the submergence depth decreased, reducing the buoyant force on the sample. As a result, the sample appeared (from the balance reading) to gain more water than it actually did. This error occurs whenever imbibition is from a finite reservoir (without water-level control) and is proportional to the ratio of sample and reservoir cross-sectional area.

Evaporative loss from the reservoir also contributed to the decrease of submergence depth and hence to the artificial weight gains. The mathematical correction for the buoyant-force change, resulting from both imbibition and evaporative losses was developed

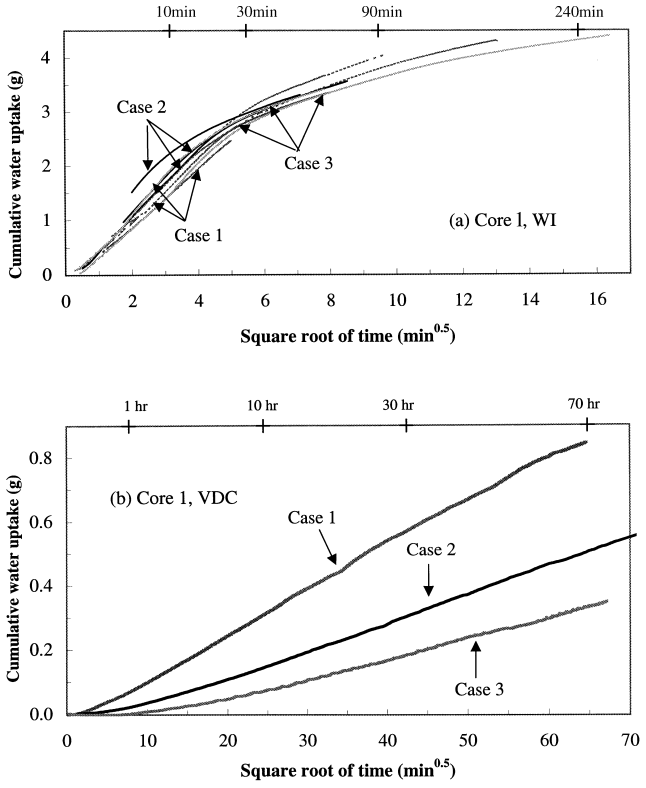

Fig. 3. Cumulative water uptake from balance indicated weights versus the square root of time for fractured Core 1: (a) WI experiments, three cases in triplicate. (b) VDC experiments, three cases.

(see Appendix A) and used to correct the experimental results to obtain true water mass imbibed into the core sample.

2.5. Water vapor diffusion and condensation experiments

In addition to liquid imbibition, samples also gain water by vapor-phase diffusion and condensation. To isolate this effect, we performed water-uptake experiments on two samples (Cores A and 1), both in contact with the water surface (WI) and suspended above it (VDC). Because the additional VDC contribution enters only through the top or sides of the sample, the bottom surface and bottom 1 mm of the sample sides were covered with aluminum foil, secured by twisted piano wire, in VDC experiments. We also covered different portions of the vapor-accessible surface of the samples to evaluate their contributions to uptake by VDC. The three cases of core treatments for the VDC experiments are summarized in Table 1.

3. Results and discussion

3.1. Reproducibility

In general, WI was measured on each sample nine times (three cases as described in Table 1, each case in triplicate). VDC was measured for Cores A and 1 three times, once for each case. Results of all WI tests on a typical unfractured sample (Core A) are shown in Fig. 2a, which exhibits good reproducibility among the imbibition tests. Cases 2 and 3, where VDC was minimized, were more reproducible than Case 1. For Case 1, where the sides of the core were not epoxy-coated, even a slight variation in the depth of core submergence among tests can lead to differences in water uptake amount, resulting from the extra

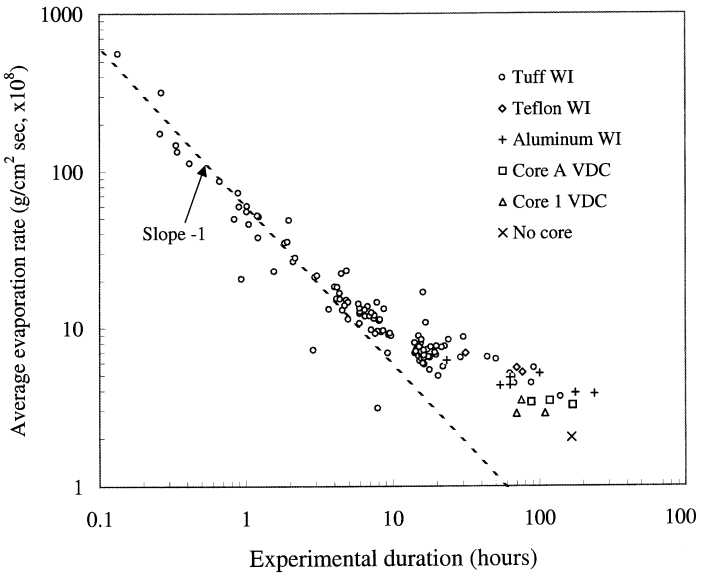

Fig. 4. Compilation of the average evaporation rate versus experiment duration for tuff rock and impermeable control samples (Teflon and aluminum).

imbibition area. For Cases 2 and 3, coating of core sides eliminated this source of variability. One-dimensional numerical simulations were performed to evaluate the effect of submergence depth. The simulations showed no detectable effect on the water uptake for core submergence depths of 0.5, 1, 2 and 4 mm for Cases 2 and 3. The uptake data for fractured Core 1 are shown in Fig. 3. The reproducibilities for different cases for fractured Core 1 (Fig. 3a) are similar to the results of unfractured Core A. From the results in Figs. 2 and 3, VDC is slow compared to WI.

3.2. Vapor phase diffusion and condensation

Water uptake by the core includes not only water imbibed but also water transported by vapor-phase diffusion into pore space and condensation in pores. For a controlled-humidity boundary condition, the Kelvin equation states that water vapor will condense inside and fill all pores smaller than a certain cutoff size, at which the meniscus curvature yields the same vapor pressure as the atmosphere (Case, 1994). The rate at which this pore-filling occurs is limited by vapor-phase diffusion through pores. Approximating the phenomenon as a one-dimensional diffusive process, the cumulative uptake of water is, at least initially, proportional to the square root of time, as shown in Fig. 2b. In other words, it would be mathematically indistinguishable from WI. Thus, the sorptivity derived from the slope of a plot of water uptake data could include the contributions of both imbibition and vapor condensation.

Comparing the water uptake by WI and VDC in Fig. 2a and b, we see that the contribution of VDC to total water uptake is significant. More water was taken up by Case 1 than by Cases 2 and 3 for VDC experiments (Figs. 2 and 3). For the unfractured Core A, the difference between Case 1 and Case 2 is approximately proportional to the accessible area. For Case 3, covering the core top causes only a slight reduction in condensation, which cannot be accounted for by the accessible core area. Significant VDC is transported into an initially dry core through the 2-mm hole because of the strong vapor pressure gradient.

Core 1 (Fig. 3a), which is fractured and contains an altered zone surrounding the fracture, imbibes water much more rapidly than unfractured Core A (Fig. 2a), making the relative VDC contribution to water uptake less significant. The VDC for fractured Core 1 is faster than for unfractured Core A, possibly due to the higher proportion of large pores in Core 1. With less

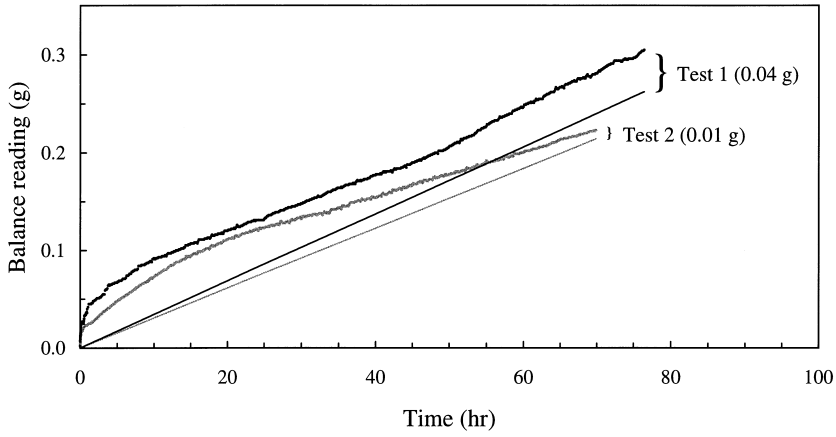

Fig. 5. Buoyancy correction for Teflon core with no imbibition for two tests.

VDC resistance within the core, the external resistance to VDC caused by the 2-mm hole is sufficient to make VDC Case 3 slower than Case 2 (Fig. 3b).

The direction of vapor-phase transport depends upon the boundary humidity and pore size. Under moderate relative humidity, water will tend to evaporate from large pores and condense in small pores. Our WI Cases 1 and 2 correspond to unjacketed and jacketed samples measured by Humphrey et al. (1996). They reported that samples with porosities greater than 0.14 gained weight slowly when unjacketed than when jacketed, and attributed this to evaporation from the core. Our samples had matrix porosity about 0.1 and gained weight faster when unjacketed. We attribute the extra weight gain to vapor-phase diffusion and condensation. Humphrey et al. (1996) also found that their least permeable sample, with porosity about 0.1, gained weight faster when unjacketed, which is consistent with our findings.

Discussion thus far on the water uptake is based on the direct balance readings. We now derive corrections to balance readings to account for evaporative loss and change in buoyant force during the experiments.

3.3. Evaporative loss from the reservoir

From independent weighings, both the mass of water imbibed and the actual mass of water remaining in the reservoir were calculated, and the sum of two quantities was always less than the initial content of water in the reservoir. The difference was attributed to evaporation from the surface of the reservoir. Evaporative loss was calculated from mass balance analysis and normalized to the annular area available for evaporation to obtain the evaporative rate. Fig. 4, a compilation of 134 experiments, shows the decrease of duration-average evaporative rates for longer experiments, which was the same for both WI and VDC experiments. Data points for Teflon and aluminum cores in Fig. 4 agree with data for tuff cores. Fig. 4 shows an initial slope of -1, approaching a quasi-constant rate after about 30 h. This is consistent with the transient evaporation process caused by an initial humidity deficit, resulting from opening the chamber to place the sample inside. At long duration, the small quasi-steady-state evaporative loss from the chamber is maintained through the hole that the balance wire passes through.

3.4. Balance reading correction for buoyant force change

During imbibition experiments, the level of water in the reservoir decreases because of both imbibition and evaporation. This drop in the water level results in an apparent increase in the weight of the sample because the buoyant force on the sample decreases. A direct conversion can be derived between mass of water loss from the reservoir and the resultant decrease in buoyant force. From the core diameter

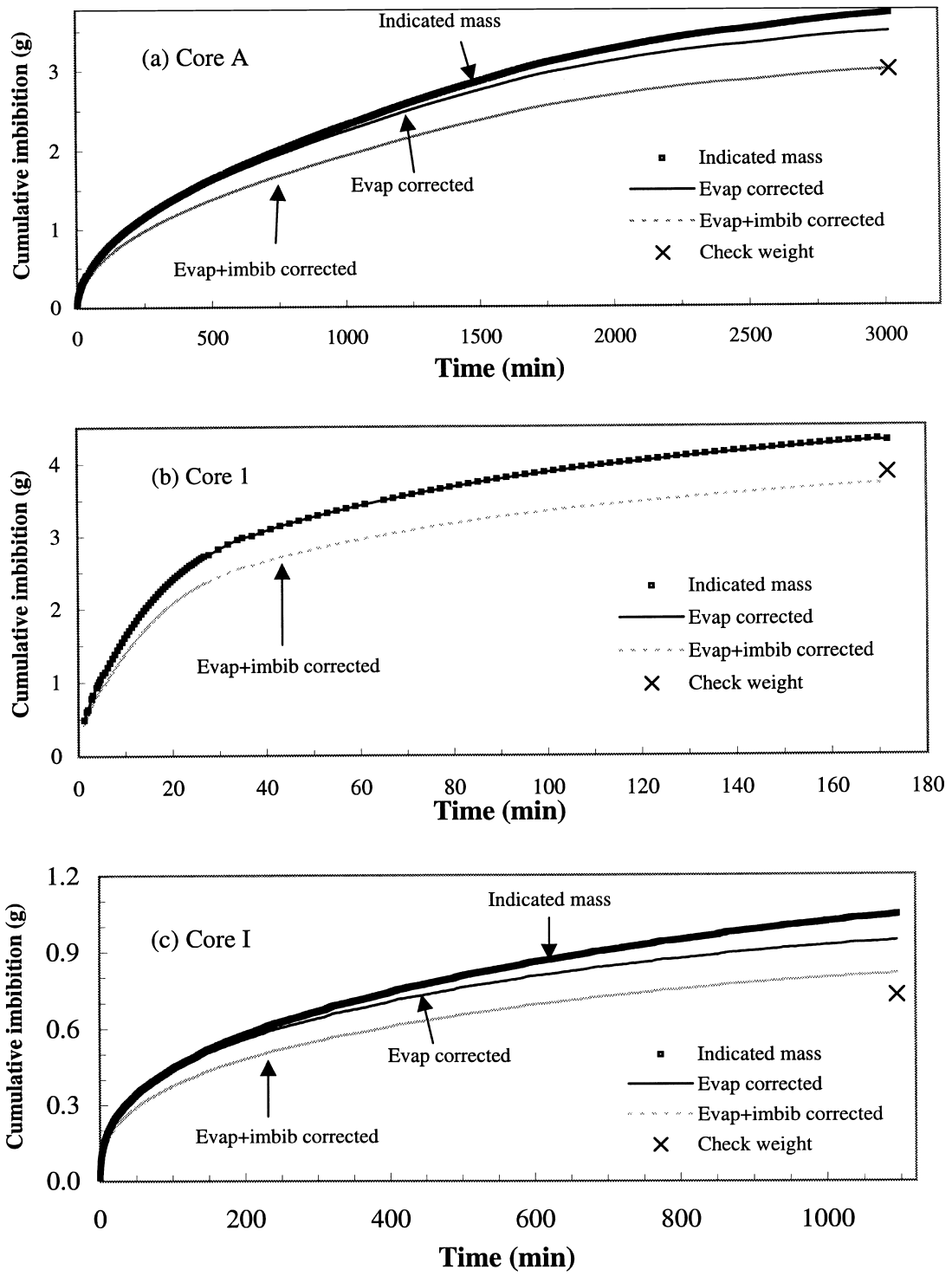

Fig. 6. Water imbibition into rock cores presented as cumulative imbibition vs. time: (a) unfractured Core A; (b) fractured Core 1; and (c) unfractured Core M with the initial core saturation of 76%.

(5.08 cm), reservoir diameter (13.66 cm), and water density (1 g cm^{-3}), it is found that 1 g of water loss from the reservoir is equivalent to 0.079 mm submergence depth decrease, which causes 0.160 g apparent uptake of water.

To further evaluate the effect of buoyant-force change and correction formulation, we conducted WI experiments using a Teflon core 4.8 cm in diameter and 2.5 cm long. Independent weighings of the core at the beginning and end of the experimental runs showed no weight change in the core. Thus, the balance-reading increase is caused solely by the buoyant-force change from evaporative loss as shown in Fig. 5. Evaporative loss, calculated from the two reservoir weighings at the start and end of the experiment, is treated as uniform over time. The buoyancy correction, calculated according to Appendix A, agrees reasonably well with the indicated balance readings. The difference at the end of the experiments seems to result mostly from an initial jump in indicated weight during the first 10 min, after which the data are approximately parallel. Presumably, this initial jump occurred in all tests but was obscured by the water uptake for imbibing tuff cores.

The reason for this initial jump is obscure. We speculate that for water-wettable samples, the meniscus rises around the circumference of the sample, and surface tension pulls downward on the sample. Experiments with an aluminum core, more water-wettable than the Teflon, showed higher initial jumps. However, this explanation appears to be incomplete, because the initial jump for the non-wettable Teflon core experiments was small, but still positive. The small jumps are treated as residual errors in our studies.

Examples of cumulative imbibition versus time for Case 3 are shown in Fig. 6. The data presented in these figures are first plotted uncorrected, then with evaporation correction, and finally with both evaporation and imbibition correction for the buoyant-force change. The correction values are the vertical displacements between pairs of curves. Also shown is the final weighing of the core sample, which serves as a check weight and shows residual experimental error. The residual error for 107 WI runs is tabulated in Table 2. Residual error was negative more often than positive, and was greatest in magnitude for Case 1 and least for Case 3, suggesting variability in VDC contribution.

This residual error is small compared to the error caused by buoyancy effects, which always overestimates sorptivity. Table 2 shows that this was generally about 20%. Therefore, correcting for buoyant-force effects eliminates 90% or more of the error in measuring the actual water uptake into the rock core. Residual error (initial jump and experimental error of weighing) is approximately similar among experiments, but its relative weight is greater for samples with small available porosity, such as unfractured Core M with 76% initial saturation (shown in Fig. 6c).

Errors from imbibition and evaporation can be minimized but not eliminated entirely. Humphrey et al. (1996) observed buoyancy effects for values of submergence depths between 1.6 and 12.7 mm. They controlled the effects by using the same initial value of submergence depth s for all runs, and assumed s to be unaffected by either imbibition or evaporation. Minimizing the ratio of sample to reservoir area reduces buoyancy effects. Humphrey et al.

Table 2
Errors before and after corrections

Case	Error caused by buoyancy effects[a]	Direction of residual error[b], number of runs		Residual error[b] (%)
	Mean and Std. Dev.	Positive	Negative	Mean and Std. Dev.
1	20.30 ± 2.21	12	18	− 2.35 ± 8.90
2	19.87 ± 1.64	7	16	− 1.24 ± 2.75
3	21.43 ± 2.32	27	27	0.00 ± 0.05

[a] Error caused by buoyancy effects (always positive) is (water uptake from indicated balance reading − water uptake from corrected balance reading)/(water uptake from corrected balance reading), expressed as a percentage.

[b] Residual error is (water uptake from corrected balance reading − water uptake from check weight)/(water uptake from check weight), expressed as a percentage.

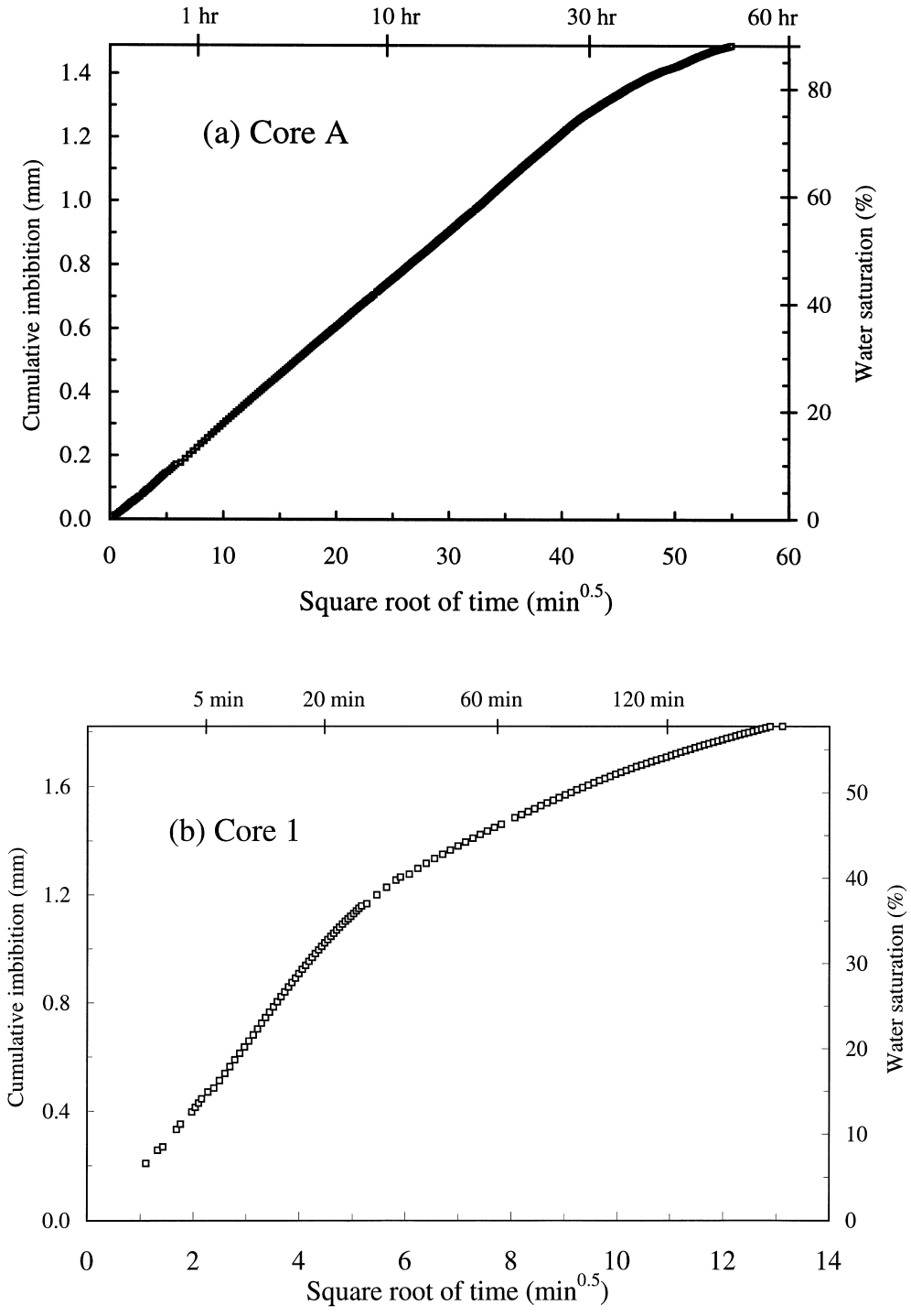

Fig. 7. Relationship of cumulative imbibition and water saturation vs. the square-root of time: (a) unfractured Core A; and (b) fractured Core 1.

Table 3
Summary of measured hydrologic properties for core samples

Core ID	Core A	Core B	Core C	Core 1[a]	Core 2[a]
Porosity ($cm^3\ cm^{-3}$)	0.082	0.086	0.082	0.160	0.104
Bulk density ($Mg\ m^{-3}$)	2.23	2.23	2.27	2.24	2.22
S, Case 1 ($\mu m\ s^{-0.5}$)	4.07 ± 0.088	5.09 ± 0.13	5.13 ± 0.11	31.47 ± 2.40	9.97 ± 0.46
S, Case 2 ($\mu m\ s^{-0.5}$)	3.57 ± 0.22	4.72 ± 0.046	4.79 ± 0.16	36.56 ± 2.86	8.69 ± 0.34
S, Case 3 ($\mu m\ s^{-0.5}$)	3.58 ± 0.058	4.41 ± 0.098	4.43 ± 0.014	33.95 ± 2.57	8.44 ± 0.55
VDC Contribution[b] (%)	13.8	15.4	15.8	−7.3	18.2

[a] Sorptivities calculated for fractured cores are apparent values.
[b] (Case 1−Case 3)/Case 3.

(1996) achieved a small ratio of sample to reservoir area by using smaller samples and tested several samples simultaneously, with each reservoir connected via a submerged siphon to a master reservoir with large surface area. With multiple samples and a large master reservoir, mass balance measurements cannot be made for correction and checking. We adopted the finite reservoir approach, which permits us to measure and correct for known errors, instead of trying to reduce the magnitude of errors. The agreement of corrected mass uptake with the check weighing confirms that this approach was justified.

3.5. Calculation of sorptivity in WI experiments

Typical plots of corrected cumulative imbibition versus the square-root of time are shown in Fig. 7. The linear segments are evident only for the "early" times, which differ between unfractured Core A and fractured Core 1. Deviation from linearity at later times can be caused by the leading edge of the wetting front reaching the top boundary (Zimmerman et al., 1990). For fractured Core 1, we saw that water was imbibed preferentially into the altered zone around the fracture, which is therefore presumably more permeable than the rest of the core (this effect was noted by

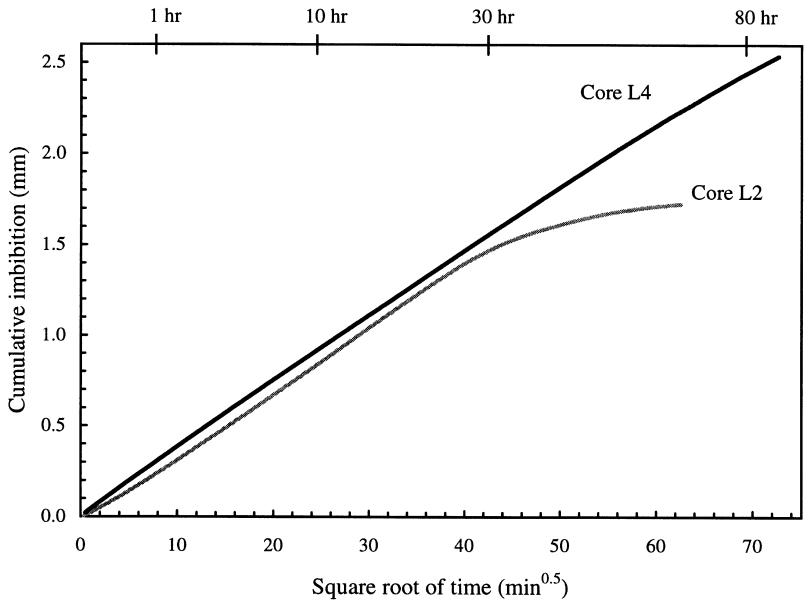

Fig. 8. Effect of core length on cumulative imbibition vs. the square-root of time. Core L2 has a core length of 2 cm and Core L4 has a length of 4 cm.

Tokunaga and Wan 1997; 2001). The measured porosity for Core 1 is 0.160, possibly due to the altered zone of larger porosity and permeability near the fracture, compared to 0.0821 for Core A (Table 3). Once this zone was sufficiently saturated, horizontal imbibition into the less permeable unaltered tuff began. This may be the cause of the slight increase in slope at 5 min (Fig. 7b). Imbibition in the fractured Core 1 is more complicated than one-dimensional process, and the linear slope should be treated as the "apparent" sorptivity. The visible wetting front reached the top of the core after 20 min, which corresponds to the time when the curve starts to bend over. At this time, the water saturation (water imbibed divided by whole-core pore volume) was only 35%, with most of the water in the altered zone. By comparison, wetting front propagation for unfractured Core A imbibition was much more uniform, traveling less than 0.3 cm in 30 min. For this sample, the linear segment ends after 29 h, which is likely related to the arrival of the wetting front at the top of the core. At this time, the water saturation of unfractured Core A was about 80%.

To evaluate core length effect, two cores with lengths of 2 and 4 cm (Cores L2 and L4) were machined back-to-back from a rock block, and imbibition tests were conducted. As shown in Fig. 8, for Core L2, $I(t)$ vs $t^{0.5}$ shows curvature after 30 h, whereas Core L4 show no such deviation. The L4 imbibition data deviate slightly from the linear segment at later time, which is possibly related to the heterogeneity of the core sample or increased effect of gravitational forces. The slopes of the linear portions are nearly identical, 4.66×10^{-6} m s$^{-0.5}$ for Core L2 and 4.60×10^{-6} m s$^{-0.5}$ for Core L4.

Sorptivities were determined by the slope of the linear segment from plots (Table 3). To standardize the procedure for setting the cutoff point, noisy initial points (if any, lasting less than one minute), attributed to establishment of the boundary at the lower end of the core, were eliminated. A straight line was fit to the next n points. The cutoff was set by varying n to maximize the correlation coefficient R^2. This procedure was also corroborated with the visual inspection of the data.

The ratio of vapor condensation versus imbibition into rock is as large as 10% at less than 1 h of experimental duration for Core A. The ratio is less pronounced for fractured Core 1, where significant imbibition along the altered zone near the fracture outweighs the vapor condensation contribution. The measured sorptivities are compiled in Table 3 for three cases of core coverage treatment. Between Case 1 and Case 3, the difference in measured sorptivity was between 14 and 18% (except for fractured Core 1), which is consistent with the contribution from vapor condensation to water intake.

Buoyancy change and vapor condensation are both errors that tend to overestimate the sorptivity of the sample. In these experiments, we found that their combined effects may cause a 40% overestimate of sorptivity. Since permeability is proportional to the 4th power of wetting front distance (Kao and Hunt 1996) and sorptivity (Tokunaga and Wan, 2001), this would lead to 3.8 times difference in calculated permeability. The relative importance of these errors may depend upon the sample properties and size. For rapidly imbibing samples, such as fractured Core 1, VDC uptake and buoyancy change due to evaporation are small; and for smaller samples (relative to reservoir size), buoyancy change due to uptake would be less.

Comparing sorptivity values for Core A and Core 1 can yield a general indication of the ratio of intrinsic permeability of the altered (fracture-surrounding) and unaltered tuff matrix. The average sorptivity is 3.40×10^{-5} m s$^{-0.5}$ for Core 1 (an "apparent" value) and 3.58×10^{-6} m s$^{-0.5}$ for Core A; thus the sorptivity ratio is 9.49. The 4th-power relationship between permeability and sorptivity suggests that permeability for Core 1 (specifically the permeability of the altered zone) was about 8100 times greater than that for the unfractured Core A. However, we note that the apparent sorptivity measured for Core 1 depends upon the portion of the sample occupied by the altered zone, and thus on sample size.

4. Conclusions

A well-controlled method has been developed for measuring imbibition rates and determining sorptivities for low-porosity/permeability media, which accounts for buoyancy and vapor-condensation effects. Automatically recorded balance readings were used to quantify the imbibition of water into

rock cores, even when the total mass of imbibed water was small and the duration of the experiment was long. The total uptake of water was checked against independent weighings of the sample before and after each experiment. A formulation was developed to correct for the apparent balance increase, resulting from buoyant-force decrease. Balance readings corrected for this effect agree very well with independently measured total uptake. Sorptivity is calculated from the slope of a plot showing corrected cumulative imbibition versus square root of time. Vapor condensation can significantly contribute to the water uptake into cores during imbibition experiments; rock cores were treated by coating and coverage to reduce this effect. Comparison of the sorptivity values for different core treatments consistently shows the contribution of vapor condensation influencing true imbibition measurement. Overall, methods for separating the confounding effects of buoyant-force change and vapor condensation result in more accurate measurement of sorptivity, as shown from the consistent and reproducible results from triplicate measurements. The developed method is expected to be very useful in providing high resolutions for measuring imbibition rates of materials with low available porosity, such as those with very low permeability and/or initial partial saturation. Continuing work on WI and tracer movement into partially saturated tuff, based on this method, will be presented in future publications.

Acknowledgements

The authors thank Tetsu Tokunaga of Lawrence Berkeley National Laboratory (LBNL) for suggestions and information of the imbibition equipment set-up and technical exchange on sorptivity measurements. The authors also thank Timothy Kneafsey of LBNL for constructive discussions and technical review during the course of this work. This work was supported by the Director, Office of Civilian Radioactive Waste Management, US Department of Energy, through Memorandum Purchase Order EA9013MC5X between TRW Environmental Safety Systems and the Ernest Orlando Lawrence Berkeley National Laboratory. Additional support was provided by the US Department of Energy, Assistant Secretary for Energy Efficiency and Renewable Energy, Office of Geothermal Technologies. Support from both DOE programs was provided to LBNL through the US Department of Energy Contract No. DE-AC03-76SF00098.

Appendix A. Mathematical formulation of buoyancy correction

The mathematical correction for the buoyant-force change is as follows:

Let subscript 0 indicate initial values and

A, area of the reservoir (e.g. petri dish) (m^2)
a, area of the sample (m^2)

then

$(A - a)$, free area of water (m^2)
ρ, density of water (kg m^{-3})
e, evaporation rate (kg m^{-2} s^{-1}). For simplicity, e is assumed to be constant during each experiment, although it is actually known to decrease during the experiment.

Let

$s = s(t)$, submergence depth at time t (m)
$m = m(t)$, actual mass of water imbibed at time t (kg)
$i = i(t)$, indicated mass of water imbibed at time t (kg)
g, acceleration of gravity (m s^{-2}).

The correction enables unknown $m(t)$ to be calculated from observed $i(t)$. Four forces, two upward and two downward, act on the sample at all times (Table A1). For simplicity we will operate only with the scalar magnitudes of the forces. All forces will be defined as positive. Therefore, rather than balancing forces by $\sum F = 0$, we will use $\sum F_{up} = \sum F_{down}$.

When the sample is first placed in contact with the water, it is in static equilibrium:

$$F_1 + F_2 = F_3 + F_4$$

Static equilibrium is also maintained throughout the

Table A1
Description of forces acting on the system

Up		Down	
F_1	F_2	F_3	F_4
Balance hook pulling upward on sample (indicated mass)	Water buoying up sample	Gravity acting on mass of imbibed water	Gravity acting on mass of original weight of sample
Always positive, always increasing	Proportional to $s(t)$, always decreasing always positive (ignore if $s < 0$)	Always positive, always increasing	Constant

experiment. Therefore

$$\Delta F_1 + \Delta F_2 = \Delta F_3 + \Delta F_4 = \Delta F_3$$

where Δ indicates change since time zero.

Using $F = MA$,

$$(i - i_0)g + (s - s_0)a\rho g = (m - m_0)g \tag{A1}$$

i.e.

$$\Delta i + (\Delta s)a\rho = \Delta m \tag{A2}$$

Although the forces themselves are defined to be always positive, Δs is always negative; i.e. the submerged length is decreasing.

Through a volume balance, Δs can be related to e and Δm: $(et(A - a))/\rho$ represents the cumulative volume of water lost from the reservoir by evaporation at time t (always a positive quantity). $(\Delta m)/\rho$ represents the cumulative volume of water lost by imbibition (also always a positive quantity). The sum of these two volumes, spread over the area $(A - a)$, is the drop in water level of the reservoir. Area $(A - a)$ is positive, but Δs is negative. For this reason, we introduce a minus sign before Δs in the volume-balance equation:

$$-\Delta s(A - a) = \frac{et(A - a)}{\rho} + \left(\frac{\Delta m}{\rho}\right) \tag{A3}$$

and

$$-\Delta s = \frac{et}{\rho} + \left(\frac{\Delta m}{\rho(A - a)}\right) \tag{A4}$$

Substituting Eq. (A4) into Eq. (A2), and solving for Δm,

$$\Delta i - a\rho\left[\frac{et}{\rho} + \left(\frac{\Delta m}{\rho(A - a)}\right)\right] = \Delta m \tag{A5}$$

so

$$\frac{\Delta i - aet}{\left(1 + \left(\frac{a}{A - a}\right)\right)} = \Delta m \tag{A6}$$

Eq. (A6) can be used to convert observations of Δi to Δm.

One can separate the contributions of evaporation and imbibition from the total buoyancy correction. The correction (defined to be a positive number) is $\Delta i - \Delta m$. Solving Eq. (A6) for Δm in terms of Δi, we obtain

$$\Delta i - \Delta m = \Delta m(a/(A - a)) + aet$$

$$= a(\Delta i - aet)/A + aet \tag{A7}$$

where the two terms on the right-side of the equation represent the buoyancy corrections resulting from imbibition and evaporation, respectively.

References

Case, C.M., 1994. Physical Principles of Flow in Unsaturated Porous Media. Oxford University, New York.

Flint, L.E., 1998. Characterization of hydrogeologic units using matrix properties, Yucca Mountain, Nevada. Water-Resources Investigations Report 97-4243, US Geological Survey, Denver, Co.

Humphrey, M.D., Istok, J.D., Flint, L.E., Flint, A.L., 1996. Improved method for measuring water imbibition rates on low-permeability porous media. Soil Sci. Soc. Am. J. 60, 28–34.

Jury, W.A., Gardner, W.R., Gardner, W.H., 1991. Soil Physics. 5th ed.Wiley, New York (pp. 134–135).

Kao, C.S., Hunt, J.R., 1996. Prediction of wetting front movement during one-dimensional infiltration into soils. Water Resour. Res. 32, 55–64.

Philip, J.R., 1957. The theory of infiltration: 4. Sorptivity and algebraic infiltration equations. Soil Sci. 84, 257–265.

Roberts, J.R., Lin, W., 1997. Electrical properties of partially saturated Topopah Spring tuff: Water distribution as a function of saturation. Water Resour. Res. 33 (4), 577–587.

Tokunaga, T.K., Wan, J., 1997. Fast flow of water along surfaces of unsaturated fractured rock. Earth Sciences Division Annual Report (LBNL-42452). Ernest Orlando Lawrence Berkeley National Laboratory, Berkeley, CA, pp. 21–22.

Tokunaga, T.K., Wan, J., 2001. Surface-zone flow along unsaturated rock fractures. Water Resour. Res. (in press).

Zimmerman, R.W., Bodvarsson, G.S., 1995. Estimation of hydraulic conductivities of Yucca Mountain tuffs from sorptivity and water retention measurement. Lawrence Berkeley National Laboratory Report LBL-37492, Berkeley, CA.

Zimmerman, R.W., G, S., Bodvarsson, E.M., 1990. Kwicklis. Absorption of water into porous blocks of various shapes and sizes. Water Resour. Res. 26 (11), 2797–2806.

Zimmerman, R.W., Bodvarsson, G.S., Flint, A.L., Flint, L.E. 1993. An inverse procedure for estimating the unsaturated hydraulic conductivity of volcanic tuff. Proceedings of the Fourth Annual International Conference on High-Level Radioactive Waste Management. American Nuclear Society, La Grange Park, IL, pp. 1052–1058.